The SWS Z-beam-profile for SSO tracking correction

Prepared by: Bart Vandenbussche (SIDT/KUL)

1 introduction

The ISO Solar System Object (SSO) tracking was implemented as a series of one-dimensional rasters. The sampling is done in such a way that the SSO is never more than 1 arc second away from the actual pointing. This means during one raster step, the object moves over part of the beam profile, thus sampling the top of the beam profile over typically 2 arc seconds. The signal change during one raster step because of this is difficult to disentangle from the signal change because of spectral features. The detailed characterization of the relevant part of the beam profile can therefore not be derived from normal observations. We therefore performed a series of pointed observations on Titan. This note describes the purpose, implementation and first results of these observations.

2 Observation strategy

The idea behind the observations is fairly simple : keep the SWS grating scanners fixed at a relevant LVDT, point to a position on the orbit of Vesta some minutes before Vesta will arrive at that position, let Vesta pass through the SWS slit, and repeat the same procedure for enough LVDT positions to characterize all AOT-bands in at least 2 grating positions.

3 Implementation

In total 11 observations were needed to sample all AOT bands in at least 2 LVDT positions close to the band borders. Table 1 shows what SW and LW grating positions were chosen for the 11 observations (AEL - AEV). Position 5450 in Aperture 1 was chosen because this was the position at which the test on NML-CYG was done to see how much the fringes in band 3a shift when one moves away from the source in Z-direction. In band 3 a change in the signal could be caused by moving up or down at the side of a fringe.

The observations as described above were successfully performed. Table 2

4 Preliminary data analysis

4.1 Standard OLP processing up to SPD

Observations were processed up to SPD stage. As expected, SW section data have a very low S/N.

Aperture 1							
Band	borders (LVDT)		AEL	AEM	AEN	AEO	
1a	3578 - 2793	SW	5000	3950	3550	2800	
1b	5001 - 3939						
3a	6200 - 3843	LW	6200	5450	4750	3850	
Aperture 2							
Band	borders (LVDT)		AEP	AEQ	AER	AES	AET
1d	3936 - 2634	SW	7050	5700	4800	3900	2700
1e	5590 - 4679						
2a	4801 - 2681						
2b	7065 - 5689						
3c	3867 - 2252	LW	7250	6250	5300	3850	2250
3d	7294 - 5259						
Aperture 3							
Band	borders (LVDT)		AEU	AEV			
2c	5668 - 1415	SW	5650	1450			
/hline 3e	5255 - 4872						
4	4969 - 496	LW	4950	500			

Table 1: Choice of grating positions in order to sample all AOT bands close to their band borders. Per observation (AEL - AEV) a combination of a relevant SW LVDT and LW LVDT was chosen.

4.2 Conversion from Signal/ITK to Signal/offset

Per raster step the ITK of the middle of the scan was determined. For every data point in the raster step the relative ITK was then calculated:

$$itk_r el = itk - itk_m id$$

The offset of Vesta in Z-direction at a given point is then

$$offset = itk_r el * speed_z$$

The speed in Z-direction is easily obtained by using the IA-routine radec2zy and two positions of Vesta on the sky. The roll-angle of the observations was 245.49.

4.3 pointed coordinates vs actual Vesta position

The observations were so-called fixed-time. The accuracy of both coordinates in PGA and the times of scheduling is rather poor when looking at a fast moving object like Vesta. Therefore, we will have to correct the obtained offsets of Vesta with the difference between the pointed coordinates and the actual position of Vesta at the middle of the observation. Table 3 shows the times of the middle of the observation, together with the coordinates of Vesta at that time. Table 4 shows the

OLP ID	Band	LVDT
76900401	1a	3550
76900501	1a	2800
76900201	1b	5000
76900301	1b	3950
76900901	1d	3900
76901001	1d	2700
76900801	1e	4800
76900701	1e	3550
76900801	2a	4800
76900901	2a	3900
76901001	2a	2700
76900601	2b	7050
76900701	2b	5700
76901101	2c	5650
76901201	2c	1450
76900201	3a	6200
76900301	3a	5450
76900401	3a	4750
76900501	3a	3850
76900901	3c	3850
76901001	3c	2250
76900601	3d	7250
76900701	3d	6250
76900801	3d	5300
76901101	3e	4950
76901101	4	4950
76901201	4	500

Table 2: Overview (with OLP product numbers) of available LVDT positions in all AOT bands

tdt	T mid scan	POF style T	RA	Dec
76900201	1997 357 12:48:45	97357124845	01:18:33.71	-00:09:42.19
76900301	1997 357 13:01:53	97357130153	01:18:33.97	-00:09:38.49
76900401	1997 357 13:15:13	97357131513	01:18:34.22	-00:09:34.73
76900501	1997 357 13:28:33	97357132833	01:18:34.48	-00:09:30.97
76900601	1997 357 13:41:52	97357134152	01:18:34.73	-00:09:27.22
76900701	1997 357 13:55:11	97357135511	01:18:34.98	-00:09:23.46
76900801	1997 357 14:08:31	97357140831	01:18:35.23	-00:09:19.70
76900901	1997 357 14:21:52	97357142152	01:18:35.47	-00:09:15.94
76901001	1997 357 14:35:11	97357143511	01:18:35.71	-00:09:12.19
76901101	1997 357 14:48:31	97357144831	01:18:35.95	-00:09:08.43
76901201	1997 357 15:01:52	97357150152	01:18:36.19	-00:09:04.66

Table 3: Actual position of Vesta at the middle of the observation (observation here means part of the observation when the shutter is open)

TDT	Actual RA	Actual Dec	Pointed RA	Pointed Dec	dy	dz
76900201	1.30936	-0.161719	1.30936	-0.161778	-0.193289	0.0881274
76900301	1.30944	-0.160692	1.30942	-0.160750	-0.160060	0.152215
76900401	1.30951	-0.159647	1.30950	-0.159694	-0.138993	0.102991
76900501	1.30958	-0.158603	1.30958	-0.158639	-0.117926	0.0537666
76900601	1.30965	-0.157561	1.30964	-0.157611	-0.148982	0.107073
76900701	1.30972	-0.156517	1.30972	-0.156556	-0.127736	0.0582397
76900801	1.30979	-0.155472	1.30978	-0.155528	-0.168474	0.116432
76900901	1.30985	-0.154428	1.30986	-0.154472	-0.159043	0.032894
76901001	1.30992	-0.153386	1.30992	-0.153444	-0.190018	0.0866363
76901101	1.30999	-0.152342	1.30997	-0.152389	-0.124038	0.135791
76901201	1.31005	-0.151294	1.31006	-0.151278	0.0374185	0.0566793

Table 4: Comparison between actual position of Vesta at the middle of the observation and the pointed position. The difference is expressed in spacecraft coordinates

comparison between pointed positions and actual Vesta positions. The difference is also given in spacecraft coordinates, given a roll angle of 245.49.

For every observation, the difference in z-direction has to be added to the offsets calculated before.

5 First Results

De resulting beam profiles are shown in figures 1 to 27. The S/N in the SW section is very poor, but also in the LW section sudden jumps are seen in the signal. These could not be correlated with anything yet - the spacecraft attitude as registered in the IIPH files does not show this. It looks a lot like a sudden pointing change, but apparently the AOCS believes the S/C is not moving. Maybe confusion in the star tracker because Vesta is moving in ? Whatever the cause may be - we can also expect it in other SSO observations.

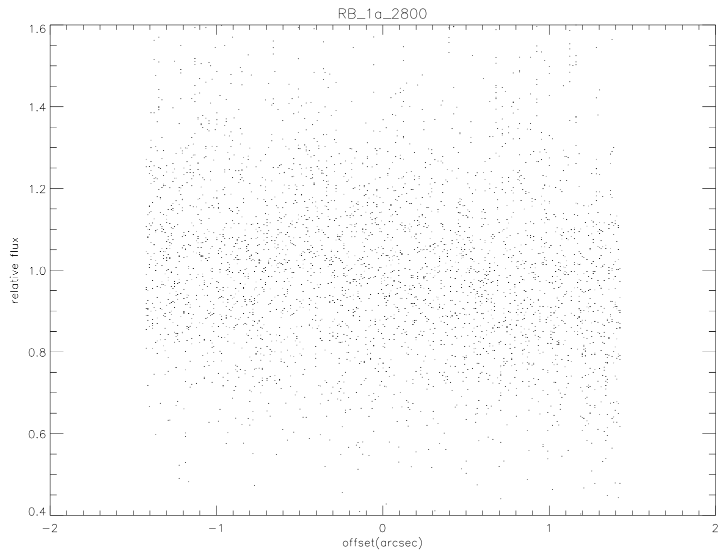

Figure 1: Signal change at LVDT 2800 band 1a

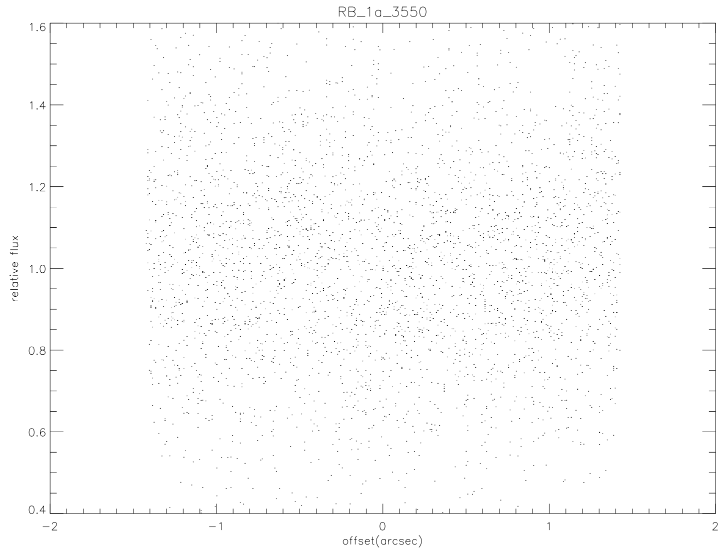

Figure 2: Signal change at LVDT 3550 (band 1a)

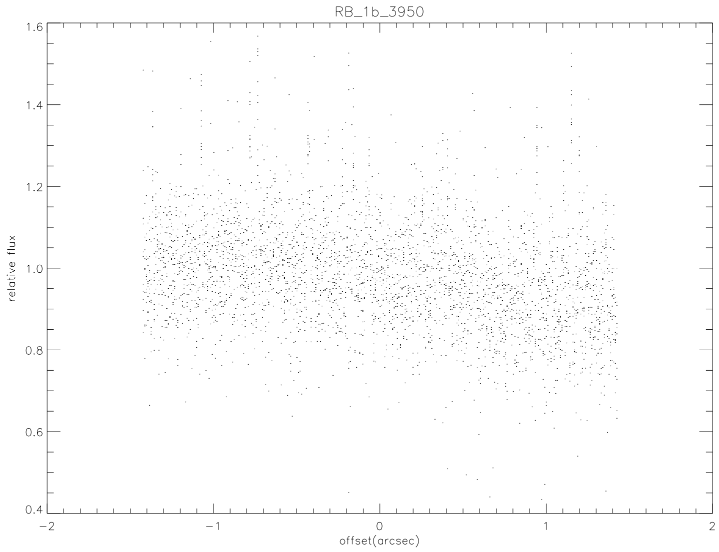

Figure 3: Signal change at LVDT 3950(band 1b)

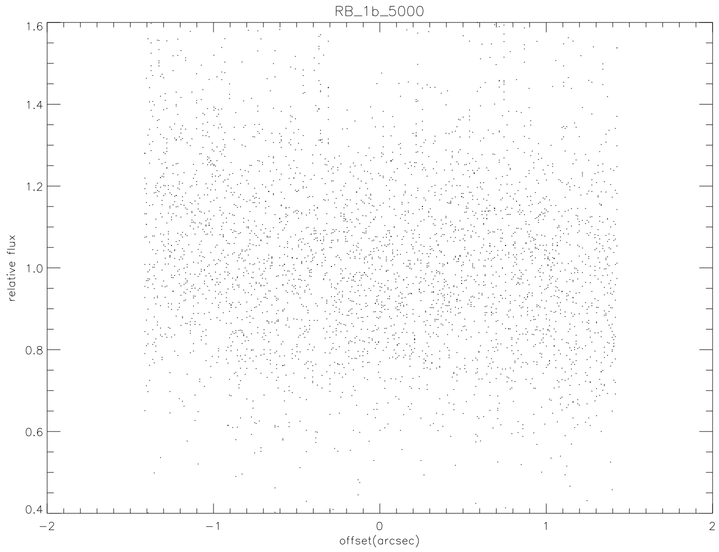

Figure 4: Signal change at LVDT 5000(band 1b)

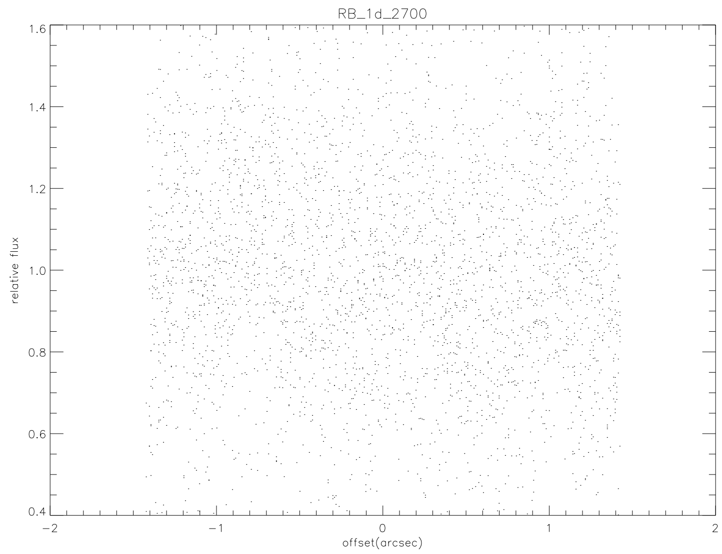

Figure 5: Signal change at LVDT 2700(band 1d)

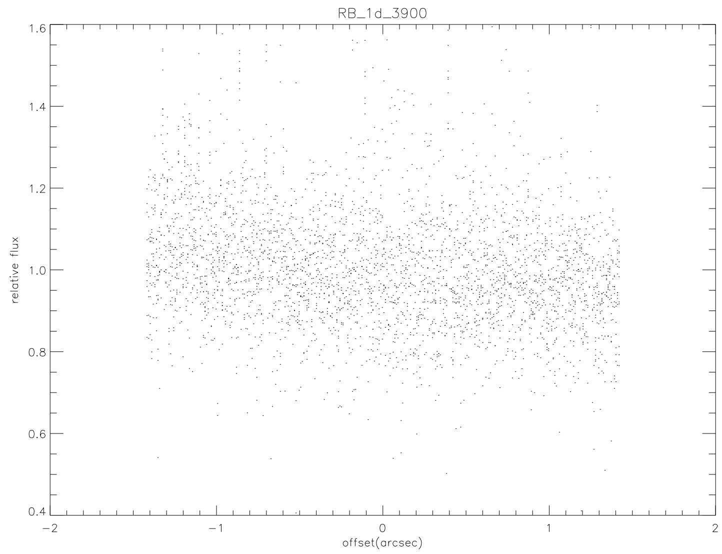

Figure 6: Signal change at LVDT 3900 (band 1d)

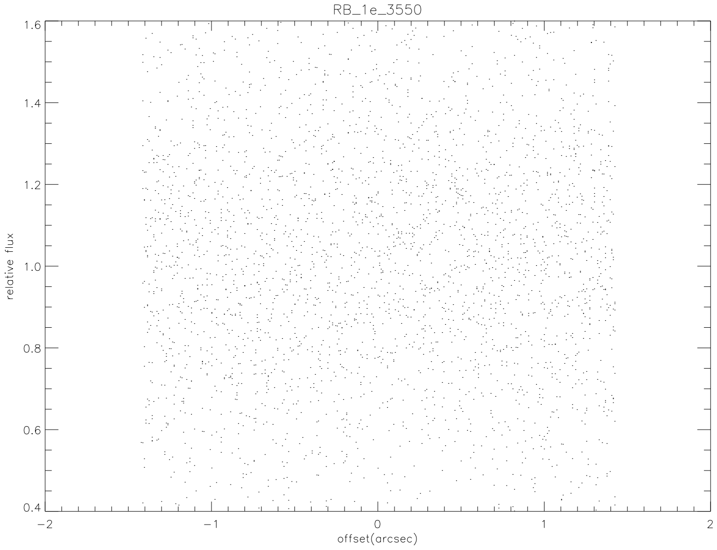

Figure 7: Signal change at LVDT 3550 (band 1e)

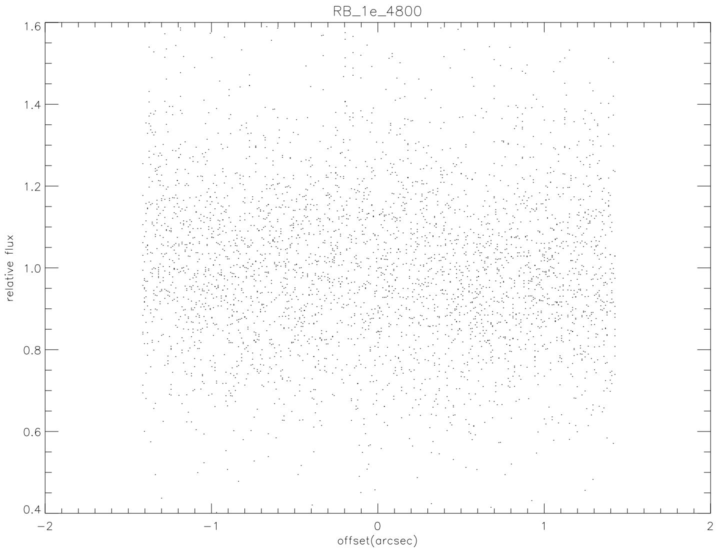

Figure 8: Signal change at LVDT 4800 (band 1e)

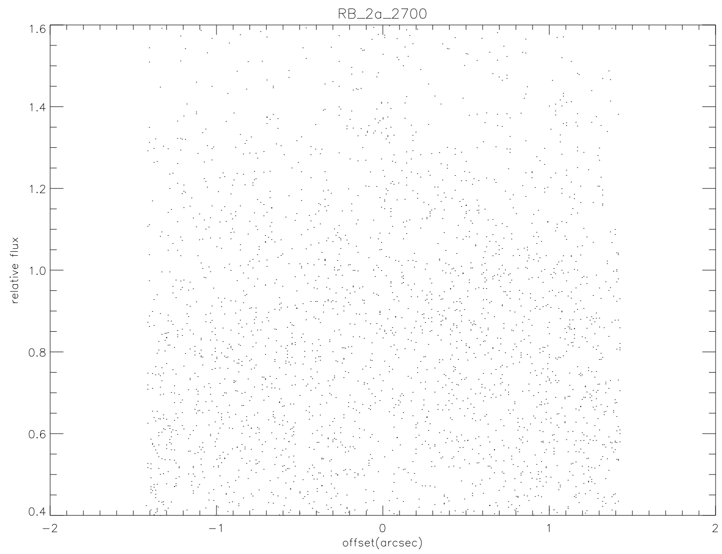

Figure 9: Signal change at LVDT 2700 (band 2a)

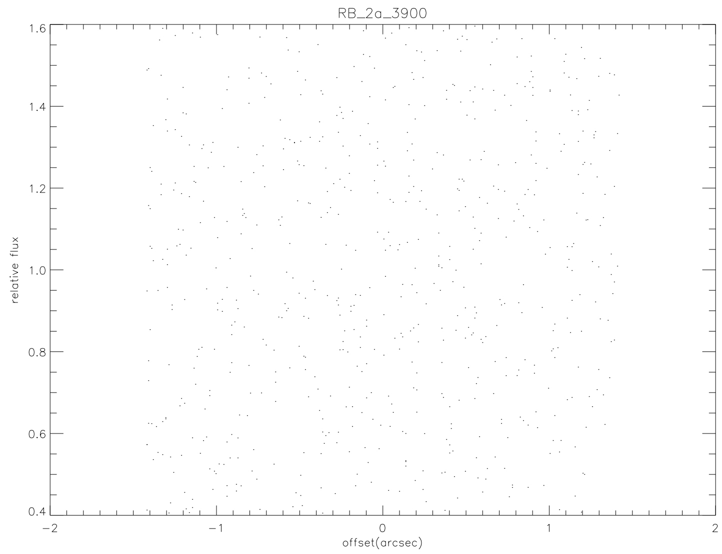

Figure 10: Signal change at LVDT 3900 (band 2a)

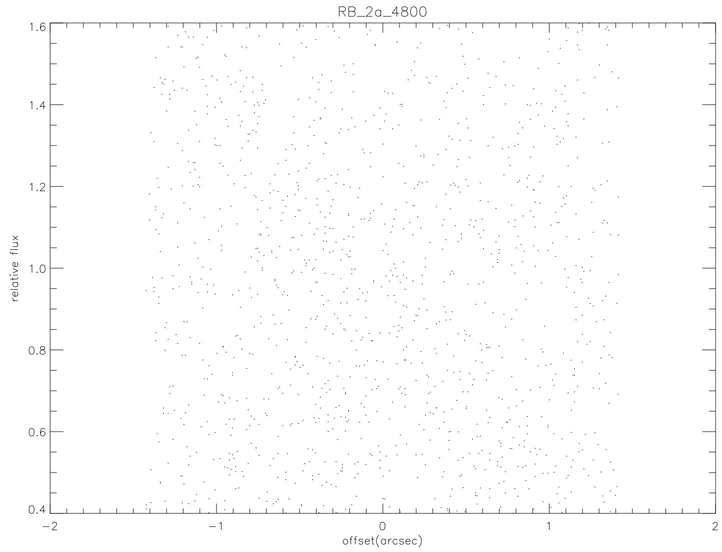

Figure 11: Signal change at LVDT 4800 (band 2a)

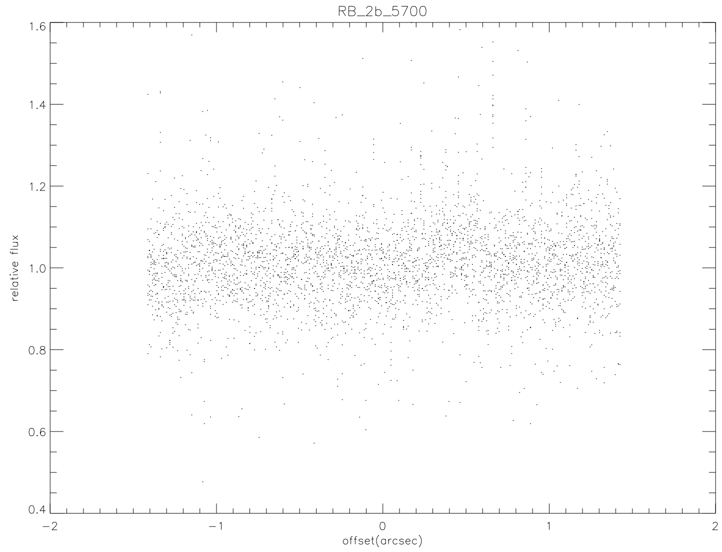

Figure 12: Signal change at LVDT 5700 (band 2b)

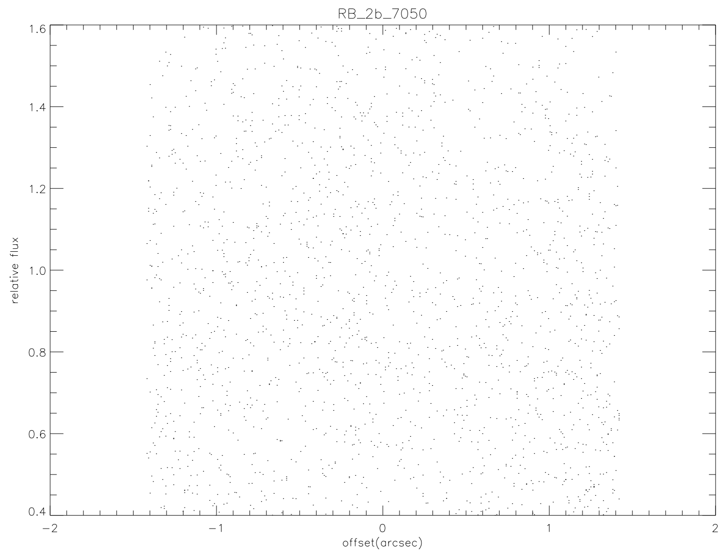

Figure 13: Signal change at LVDT 7050 (band 2b)

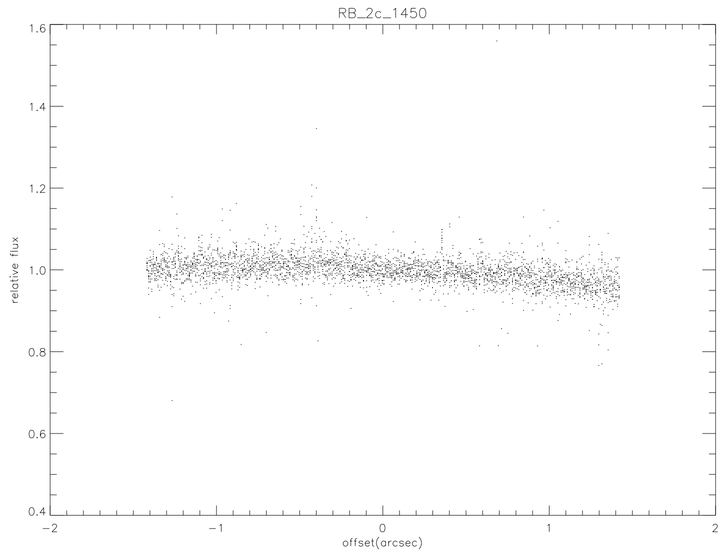

Figure 14: Signal change at LVDT 1450 (band 2c)

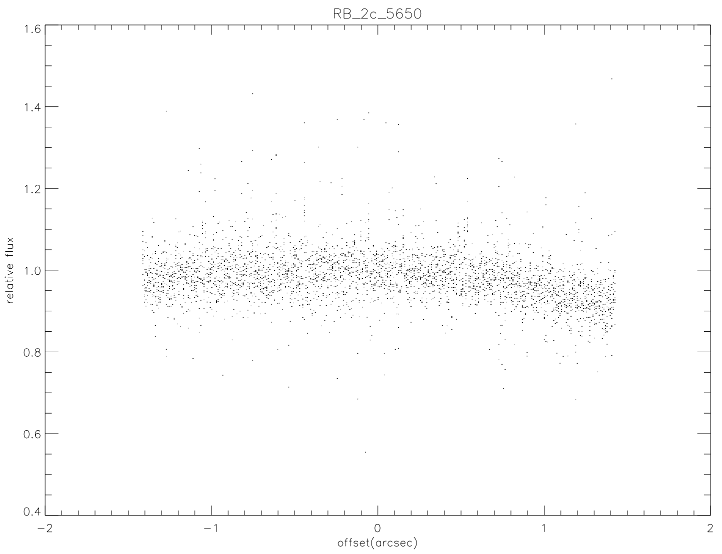

Figure 15: Signal change at LVDT 5650 (band 2c)

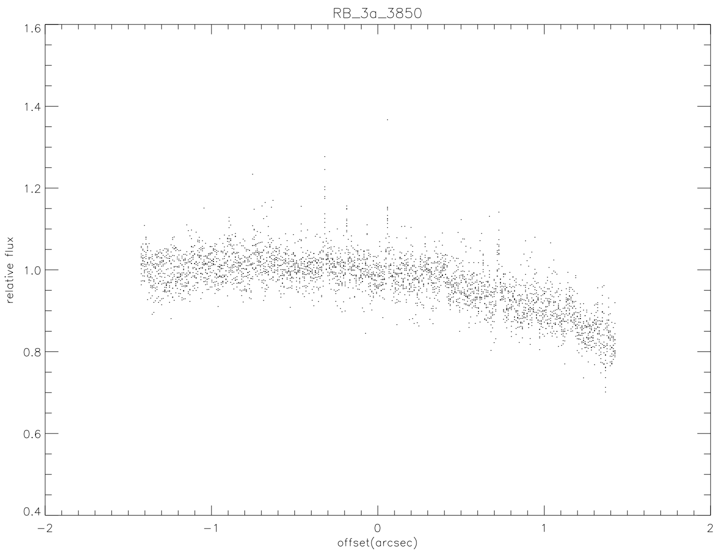

Figure 16: Signal change at LVDT 3850 (band 3a)

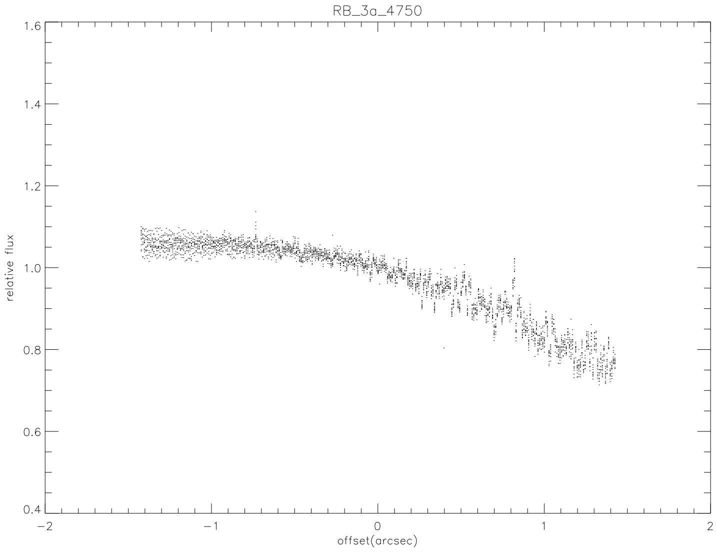

Figure 17: Signal change at LVDT 4750 (band 3a)

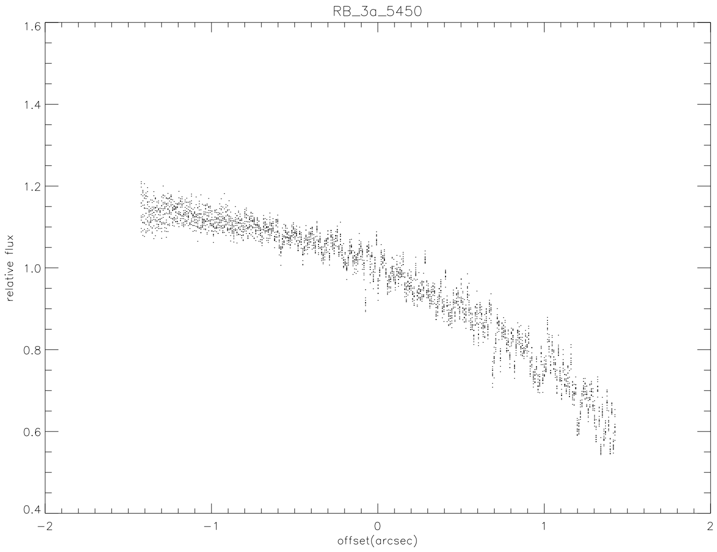

Figure 18: Signal change at LVDT 5450 (band 3a)

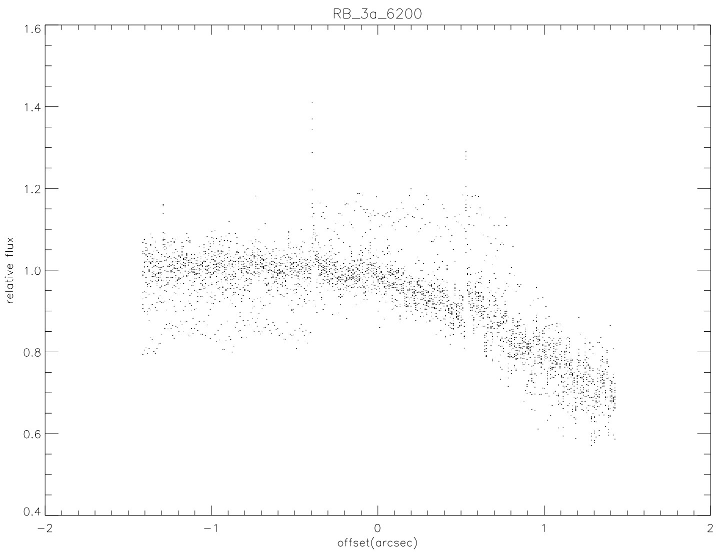

Figure 19: Signal change at LVDT 6200 (band 3a)

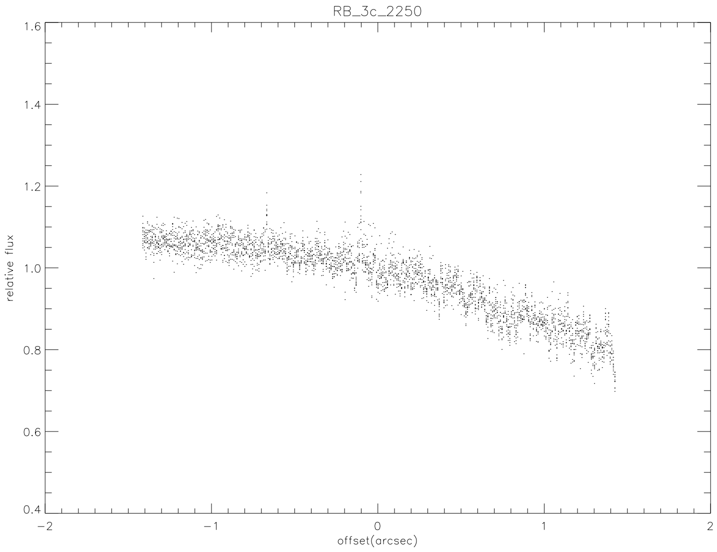

Figure 20: Signal change at LVDT 2250 (band 3c)

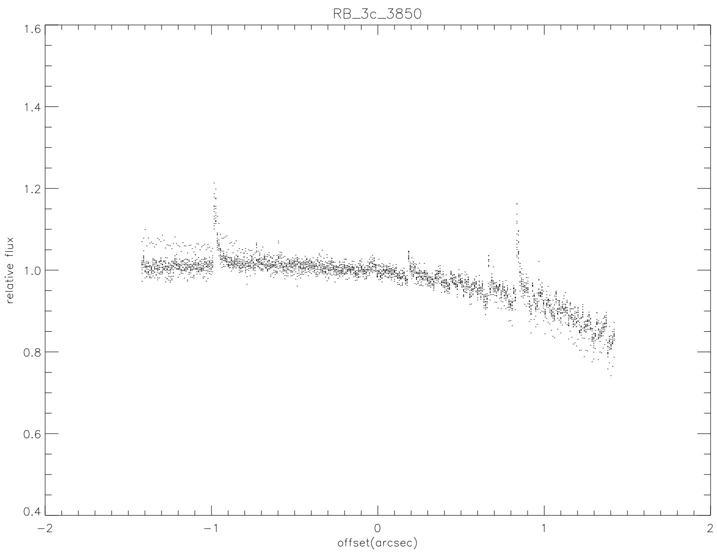

Figure 21: Signal change at LVDT 3850 (band 3c)

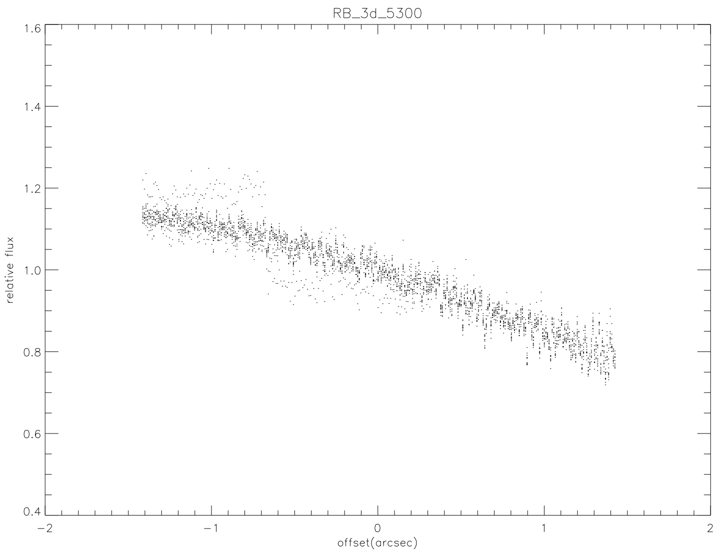

Figure 22: Signal change at LVDT 5300 (band 3d)

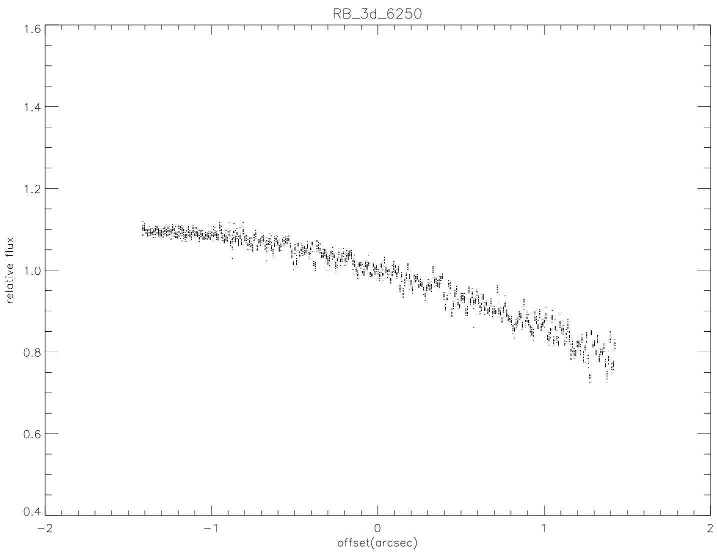

Figure 23: Signal change at LVDT 6250 (band 3d)

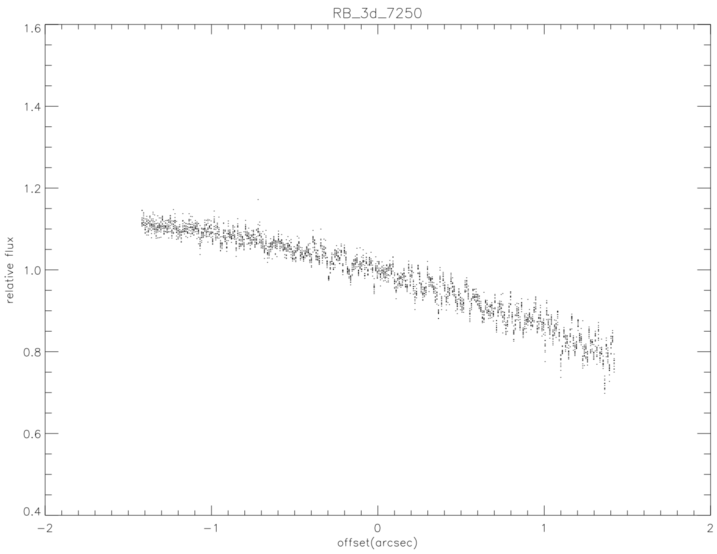

Figure 24: Signal change at LVDT 7250 (band 3d)

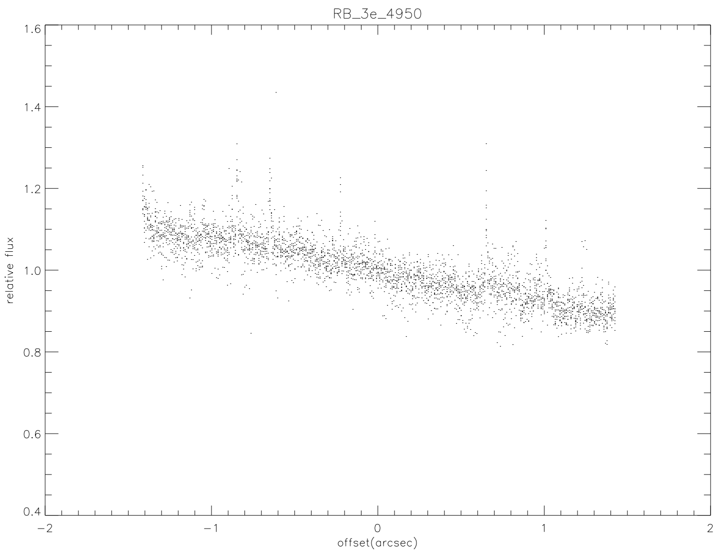

Figure 25: Signal change at LVDT 4950 (band 3e)

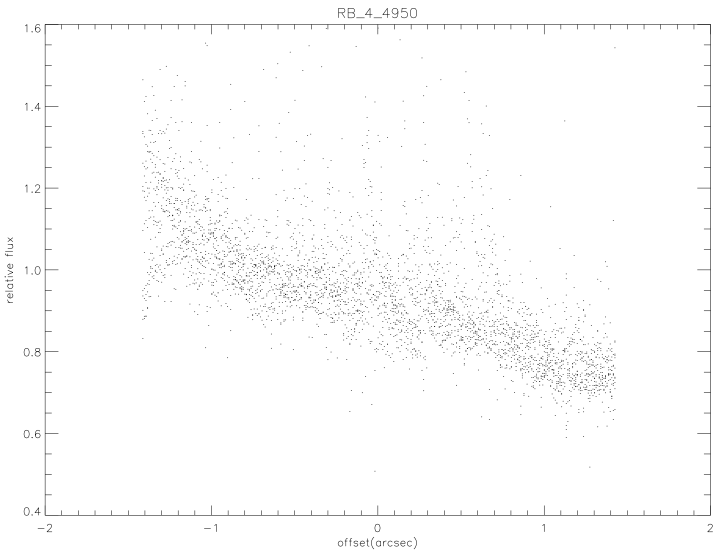

Figure 26: Signal change at LVDT 4950 (band 4)

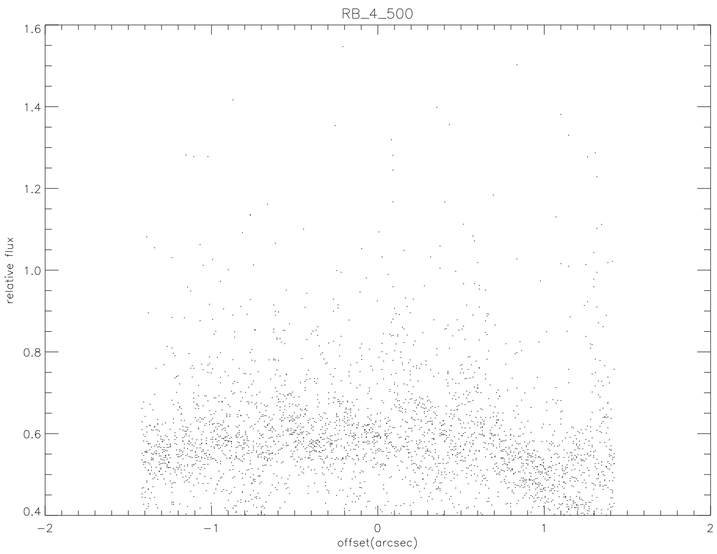

Figure 27: Signal change at LVDT 500 (band 4)

6 Comparison to other Beam profile data

No systematic comparison between the results obtained and other beam profile data was made yet, but some sporadic cases look promising. Figure 28 shows a comparison between the change in signal as Vesta crosses the SWS slit and the beam profile as derived from a 2 arc second raster on Alfa Boo for band 3C.

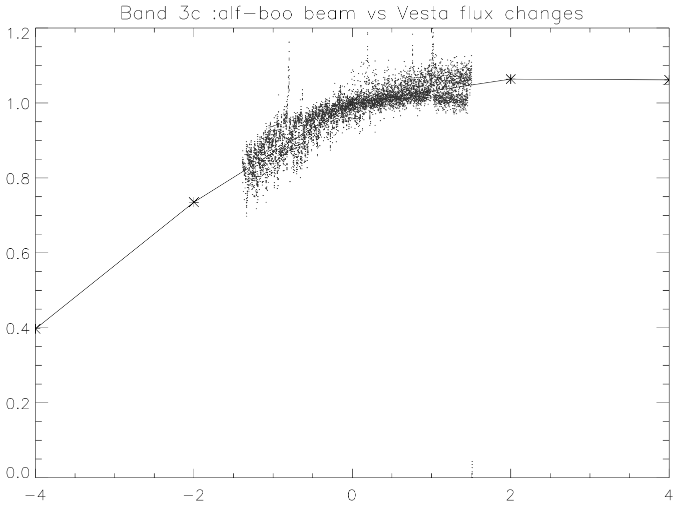

Figure 28: Comparison between the change in signal as Vesta crosses through the SWS slit and the beam profile as derived from a 2 arc second raster on Alfa Boo for band 3C.

7 Outlook

The obtained data can certainly be used to characterize the top of the beam profile in detail. This detailed characterization is needed in order to correct SSO tracking steps in SWS SSO observations.

A minimization algorithm might be needed to determine the offset of the SSO at the middle of the raster step from the actual pointing of the raster step, since this seems not to reproduce very well. Different pointing error issues might as well play a role, and should be incorporated in the processing of the observations described above.